Urban Climate xxx (xxxx) xxx–xxx

Contents lists available at ScienceDirect

Urban Climate

journal homepage: www.elsevier.com/locate/uclim

Evaluation of albedo enhancement to mitigate impacts of urban heat island in Rome (Italy) using WRF meteorological model

Elena Morini[a,*], Ali Gholizade Touchaei[b], Federico Rossi[a], Franco Cotana[a], Hashem Akbari[c]

[a] University of Perugia, Engineering Department, CIRIAF, Via G. Duranti 67, 06125 Perugia, Italy
[b] AMESiS Energy Inc, Canada
[c] Concordia University, 1455 De Maisonneuve Blvd. W., Montreal, QC, Canada

ARTICLE INFO

Keywords:
UHI
Urban Heat Island
Urban climate simulation
WRF

ABSTRACT

The extreme effects of urban heat island (UHI) on energy consumption, air quality, and human health are significantly detrimental. Increasing the albedo of urban surfaces has been proposed as a potentially efficient mitigation strategy. In this study the Weather Research and Forecasting (WRF) mesoscale model has been used to simulate the urban climate of Rome (Italy).Four different scenarios have been analyzed: the Base Scenario as control case; the Base-ALB Scenario, in which the albedo of roof, walls and road have been increased; the Morph Scenario in which the morphology of urban area has been parameterized more accurately; the Morph-ALB Scenario in which the urban albedo of the improved model has been increased.

This study demonstrates that a more accurate parametrization of the urban morphology leads to a more accurate representation of UHI phenomenon. The simulation results show that albedo increase leads to the decrease of the 2-m air temperature at day-time and at night-time. Albedo increase offers very promising results in terms of UHI mitigation, reducing the temperature in the urban area by up to 4 °C at daytime and a little increased (up to 1 °C) in some locations at night time, compared to the control cases.

1. Introduction

Since 753 BCE (the year of the founding of Rome) the land-use and the land-cover has undergone substantial changes in the region where the city is located. Today, Rome is one of the largest and most populated cities in Italy and the human settlements have replaced rural, natural areas with urban, concrete areas. As proved by several researches, human-induced landscape changes have many impacts on local and regional-scale climate (Kaufmann et al., 2007; Golden, 2010; Morini, et al 2017a). The most documented effect linked to urbanization is the urban heat island (UHI) phenomenon, that characterizes the air above the urban canopy that is usually warmer than the air in the rural surroundings.

The UHI appears in almost every urban area, no matter whether the specific city is small or large, or whether it is situated in a warm or a cold climate (Stewart and Oke, 2012). One major effect of UHIs on human health is the increase of human discomfort because of urban heat stress. UHIs increased temperatures can potentially increase the magnitude and duration of heat waves within cities (Tan et al., 2010). The relationship between the heat island and "death island" has been introduced by Buechley et al. (1972) that found the mortality rate during a heat wave increases exponentially with the maximum temperature; an effect that is enhanced

* Corresponding author.
E-mail addresses: morini@crbnet.it (E. Morini), federico.rossi@unipg.it (F. Rossi), cotana@crbnet.it (F. Cotana), HAkbari@encs.concordia.ca (H. Akbari).

http://dx.doi.org/10.1016/j.uclim.2017.08.001
Received 16 November 2016; Accepted 2 August 2017

by the UHI. In summer 2003, the Local Health Authority of Rome assessed the negative impact of heat waves on mortality: 1094 excess deaths occurred during three major heat wave periods in 2003, an increase of 23% compared with the average annual number of deaths during 1995–2002 (Centers for Disease Control and Prevention, USA, 2004).

Discomfort situations that lead to the risks to human health and the increase in mortality have been discussed by Sakka et al. (2012). Indoor thermal field measurements showed how the heat wave emphasized by UHI made people exposed to hot spells above 33 °C for 6 days continuously, provoking not only low indoor comfort issues, but also increasing the risk of non-negligible health disease for the most vulnerable households (Sakka et al., 2012). To mitigate the mortality rate, (Rossi et al., 2015c) investigated integrated aspects of comfort conditions of people in urban public environments and proposed solutions to reduce the effect of UHI.

Several studies have assessed the impact of the UHI on other aspects such as energy consumption and air quality. Elevated temperatures in fact lead to an increase in energy demand for cooling. Akbari and Sezgen (1992) found that the increase of energy demand for summer cooling is increased by 1.5–2% each 0.54 °C of temperature. According to Santamouris (2016), energy consumption for cooling represents about 2.9% to 6.7% of the total world energy consumption to date. Energy consumption for cooling will increase in the near future for combination of many factors: the global climate change, the higher temperatures in the built-up environment due to the UHI, the expected population increase and the economic development. Many researches assess that in the future cooling energy demand of buildings will very likely become the dominant energy component. At the same time the increase of energy consumption will lead to a higher amount of energy production by fossil-fueled power plants (Akbari, 2005) and systems (Rossi et al., 2015b) which lead to higher emissions of heat-trapping greenhouse gases such as carbon dioxide, as well as other pollutants such as sulfur dioxide, carbon monoxide and particulate matter that in turn worsen the UHI phenomenon (Fallmann et al., 2016).

Since the extreme effects of this phenomenon are significantly detrimental, many researchers have been focusing on proposing solutions to weaken the phenomenon itself or the related causes. Several researches use meteorological simulation tools to understand and analyze the UHI, such as Weather Research and Forecasting (WRF) mesoscale model, incorporating the urban canopy model (UCM) to consider multi-reflections between urban surfaces and to estimate the energy budget of the canopy (Ramamurthy et al., 2015; Touchaei and Akbari, 2015; Kondo et al., 2005; Kusaka and Kimura, 2004a, 2004b; Kusaka et al., 2001). Urban canopy models (UCMs) account for the exchange of energy and momentum between the urban surface and the atmosphere. 1D, 2D, and 3D UCMs are available for WRF. 1D model considers buildings and streets as a roughness of the surface; 2D model considers one directional infinitely-long street canyons, delimited by lines of buildings of equal width; 3D models recognizes the three-dimensional nature of urban surfaces and the fact that buildings vertically distribute sources and sinks of heat, moisture, and momentum through the whole urban canopy layer (Chen et al., 2011). Urban trees, soils and short vegetation have also been integrated into the urban canyon by Wang et al. (2013) and Ryu et al. (2016), whose models allow the development of the urban heat island mitigation strategy of enhancing urban greening.

Another worthy of investigation and potentially efficient mitigation strategy that is also implemented in WRF UCMs is based on the increase of the average albedo of urban surfaces throughout highly reflective materials for roofs, pavements and walls (Rosenfeld et al., 1995, 1998; Akbari et al., 2016; Morini et al., 2016). Researchers have also introduced, studied and tested at local scale innovative high albedo solutions including thermochromic materials (Doulos et al., 2004), directional materials (Hooshangi et al., 2015) and retro-reflective materials (Rossi et al., 2015a, 2016; Morini et al, 2017b) for UHI reduction.

In this paper, the effect of increasing urban surfaces reflectivity in Rome is simulated by using Weather Research and Forecasting (WRF) mesoscale model. The model is used to reproduce the circulation in the urban area of Rome in Pichelli et al. (2014). The configuration that better reproduced the dynamics of the urban area is chosen as physics parameters in this work. A multi-layer UCM is coupled to the mesoscale model to better estimate the momentum, heat, and turbulent kinetic energy budget of the urban canopy.

The objective of the paper is twofold: 1) Quantify the effectiveness of albedo increase in the urban area of Rome to reduce UHI and 2) Quantify the sensitivity of urban energy model to urban parametrization. The first objective is to prove the effectiveness of UHI mitigation strategies, focusing in particular on urban albedo increase, that allows a decrease of absorbed heat by urban surfaces, and decreases the surfaces and air temperatures.

The second objective is to provide a realistic estimation of morphologic characteristics of the investigated urban area to represent more accurately the geometry of urban canopy in the UCM and thus the fluxes from urban area to the atmosphere in the simulation model.

For this purpose four different simulations were carried out during four cloudless summer days in Rome during summer 2013. The simulations start on the 2nd of August at 00:00. The first 12 h are considered as initialization time to allow the model to reach stability.

Four scenarios are implemented: the control case is the Base Scenario. Results from numerical simulations at the highest resolution domain (260 m) are compared to measurements in 9 weather stations that cover a large area inside and around the urban area of Rome to validate the model. Temperatures in some urban points are also compared to temperatures in rural points to quantify the relevance of the UHI in Rome during the simulated days. In the Base-ALB Scenario the countermeasure to UHI is adopted and the reflectivity of urban surfaces is increased. Results from this simulation allow to verify the effectiveness of albedo increase strategy for the UHI reduction. A more accurate urban parametrization is provided in the Morph Scenario, where data in UCM describe more accurately the morphologic characteristics of the urban area. In the Morph-ALB Scenario the reflectivity of urban surfaces is increased in the improved parametrization scheme.

2. Materials and methods

2.1. Domain of interest

The area of interest is Rome, the capital of Italy, located in the central-western part of the Italian Peninsula. It is the most populous (2,900,000 inhabitants) and the largest (1300 km^2) city in Italy. Rome lies on both sides of the Tiber (Tevere) River, about 17 miles (27 km) from its mouth in the Mediterranean Sea. The river flows through the city in a generally north-south direction, but with several bends. Much of the area around the city was marshy until drainage and reclamation were completed early in the 20th century.

Rome is characterized by a Mediterranean climate (Köppen climate classification: Csa) (Peel et al., 2007) with cool, humid winters and hot, dry summers. The rainfall occurs during the winter months between October to January. The summer season lasts from June to September with temperatures ranging between a minimum of 14 °C to a maximum of 30 °C. The daily range of temperature averages at 14 °C. The winter season extends from December to March with temperatures varying between 3 °C to 16 °C. The months of April, May, October and November temperatures vary between 7 °C and 23 °C. Over the course of a year, the temperature typically varies from 2 °C to 32 °C and is rarely below − 2 °C or above 35 °C.

Rome being in the Mediterranean climatic region receives moderate rainfall throughout the year. Rainfall is heavy between October to January (about 40 cm). Over the entire year, the most common forms of precipitation are light rain, thunderstorms, and moderate rain. The relative humidity typically ranges from 38% (comfortable) to 93% (very humid) over the course of the year, rarely dropping below 31% (comfortable) and reaching as high as 100% (very humid). Over the course of the year typical wind speeds vary from 0 m/s to 5 m/s (calm to gentle breeze), rarely exceeding 8 m/s (fresh breeze) (WeatherSpark)

For the simulation, four two-way nested domains have been defined. The number of grids of the domains (west-east/south-north) are 100 × 100, 160 × 160, 151 × 151 and 151 × 151, with a land use resolution of 10 m, 2 m, 30 s, and 30 s, respectively ("m" denotes arc minutes and "s" denotes arc seconds). The coarser domain grid is 7066 m, and the ratio with the nested domains is 3.The inner domain has been set as 151 × 151, with the dimension of the grid of about 260 m, to cover the urban area of Rome. 35 vertical eta levels are set, with a higher concentration in the first kilometers to better represent the fluxes from the surfaces.

The domains configuration is shown in Fig. 1.

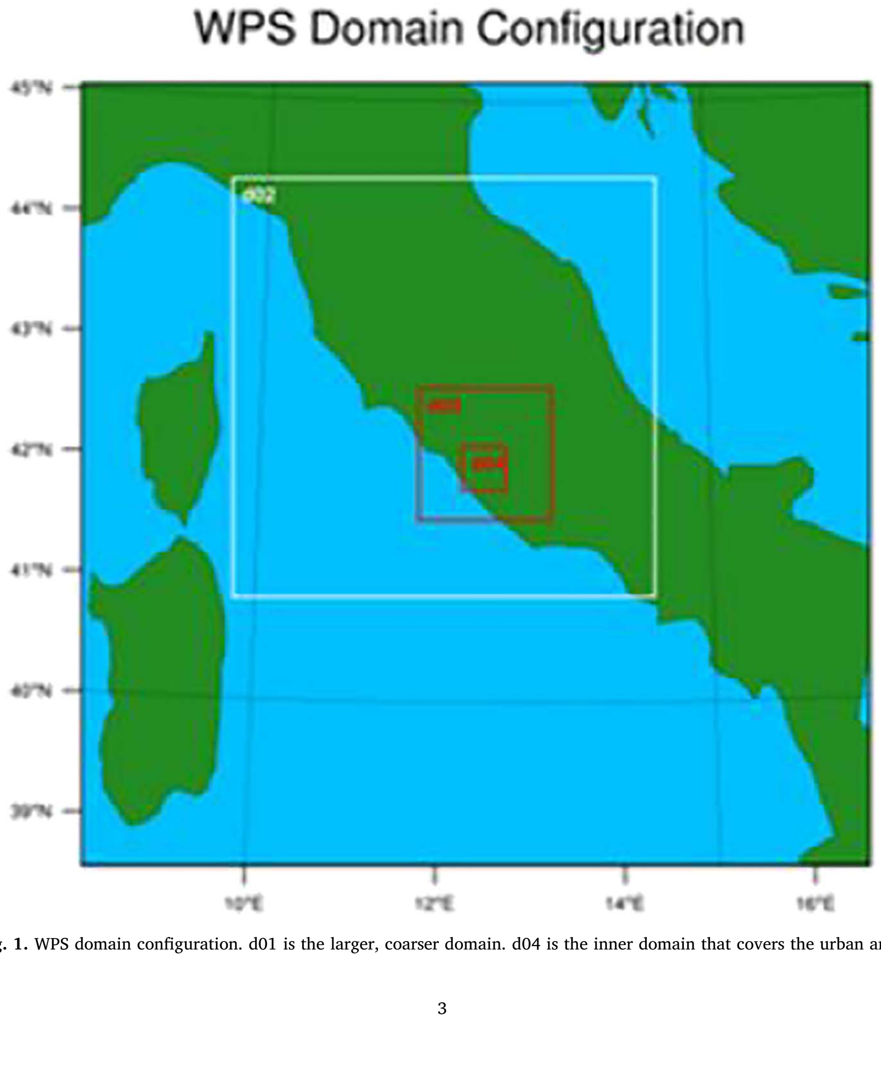

Fig. 1. WPS domain configuration. d01 is the larger, coarser domain. d04 is the inner domain that covers the urban area.

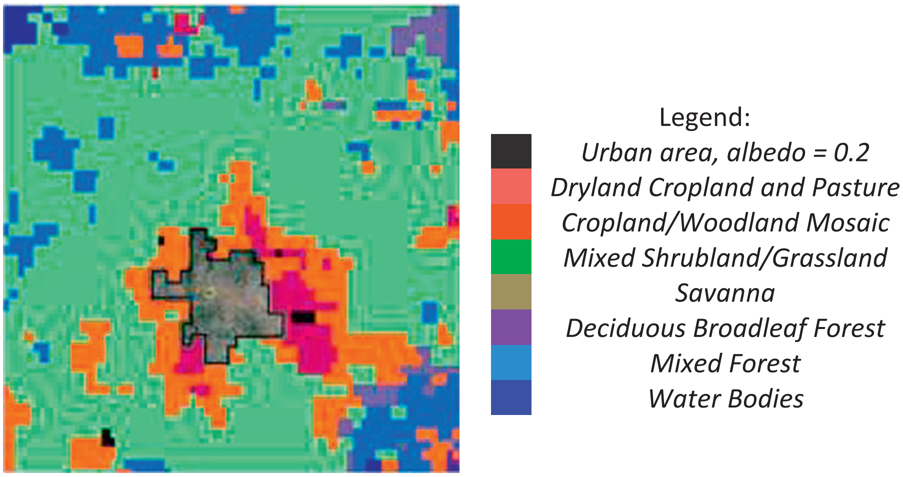

Fig. 2. Land Use for d04. Land use category data sets are matched with the USGS categories (WRF User Guide, 2009. Chapter 3).

The Land Use for the inner domain is shown in Fig. 2. The black grids cover the urban area of Rome.

2.2. Model setup

Table 1 summarizes the physics models set in the simulations. The models are

The convection of the clouds and thus the cumulus parametrization is not considered for the inner domains. The initial and boundary conditions of the simulations are determined using the ECMWF dataset (Balsamo et al., 2012) and the USGS (U.S. Geological Survey) for the weather data and the terrestrial data, respectively.

The multi-layer urban canopy model (UCM) and building energy model (BEM) are coupled to WRF model. UCM incorporates urban grids into mesoscale grids and calculates momentum, heat, and moisture fluxes from urban areas to the vertical layer of the mesoscale model. While slab and single layer UCMs consider urban areas as the roughness of the surface, multi-layer UCM divides the urban canopy into layers where building height is not constant and shading and reflected energy is estimated by the model. The BEM provides further information to the UCM, such as the building energy budget with heating and cooling systems and the heat emission from the buildings to the canopy (Touchaei and Akbari, 2015).

2.3. Scenarios

Four different scenarios are defined to study the urban temperature reduction resulted from increasing albedo of urban surfaces (i.e. roof, wall, and road). In the Base Scenario the albedo of all surfaces is 0.2, as an average values among the values by (Wärmetechnische Grundlagen der Heizungs, 1982) and default urban morphology parameters (street width, building heights, etc.) associated with the urban category have been considered representative, on average. In the Base-ALB Scenario the albedo of surfaces is set to 0.65, 0.6 and 0.45 for roofs, walls and roads respectively. The adopted values can be considered representative for highly reflective surfaces in urban area, whose albedo is influenced by daily variation due to shadowing and different sun positions. In the Morph Scenario the albedo is 0.2 and the morphologic characteristics of the urban area are set as the ones observed in the area where the reference meteorological station for urban area (Trieste-Salario, 41.935; 12.511) is located. In Section 2.5 the area is described more in detail. In the Morph-ALB Scenario the albedo is increased to 0.65, 0.6 and 0.45 for roofs, walls and roads respectively.

In order to validate of the model, the data measured by 9 weather stations located in the area of Rome have been compared to the simulated data. In Fig. 3 the location of the weather stations and in Table 2 the names and coordinates.

Table 1
Physics models configuration used in the simulations with the nonhydrostatic WRF-ARW model.

Microphysics	Morrison double-moment scheme (Morrison et al., 2009)
Longwave radiation	RRTM scheme (Mlawer et al., 1997)
Shortwave radiation	Dudhia scheme (Dudhia, 1989)
Surface layer	Eta similarity (Janjic, 2002)
Land surface	Noah Land Surface Model (Tewari et al., 2004)
Urban surface	BEM (3). Building Energy Model. (Martilli et al., 2002, Salamanca and Martilli, 2010)
Planetary boundary layer	Mellor-Yamada-Janjic scheme (Janjic, 1994)
Cumulus parameterization	Kain-Fritsch scheme (Kain, 2004)

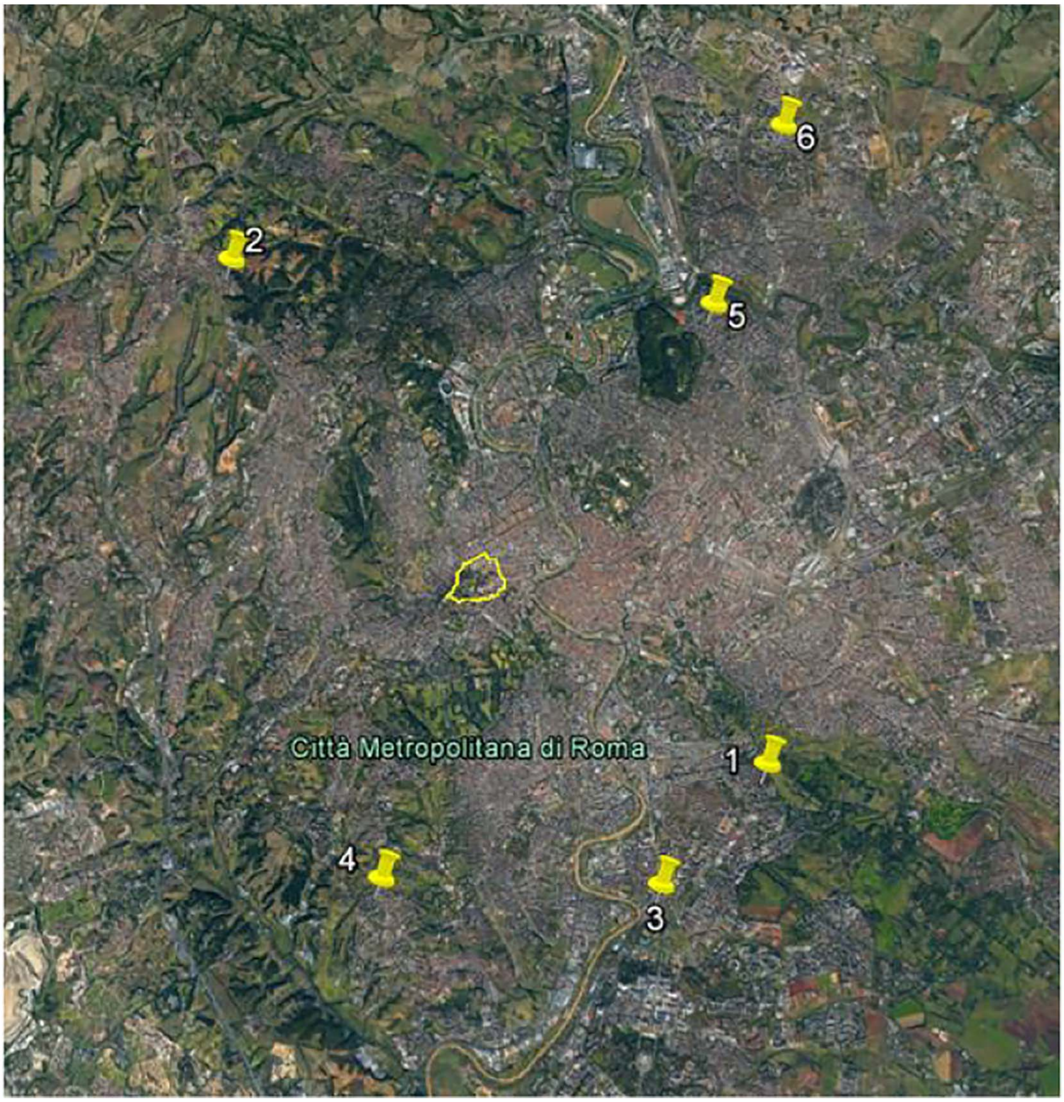

Fig. 3. Weather station locations.

Table 2
Weather stations names and location.

	NAME	LAT - LONG
1	Appia Antica Caffarella	(41.863; 12.502)
2	Collina Lanciani - Pietralata	(41.957; 12.414)
3	ILAZIORO10	(41.848; 12.475)
4	ILAZIORO28	(41.858; 12.418)
5	Trieste-Salario	(41.935; 12.511)
6	VIGNENUOVE	(41.960; 12.533)

2.4. Urban morphology

UCM allows WRF mesoscale model to establish an interaction between planet boundary level model and the urban canopy. Multi-layer UCM is the most sophisticated model that takes into account the three-dimensionality of urban surfaces and considers buildings as sources and sinks of heat, moisture and momentum. The coupling to Building Energy Model (BEM) also allows to consider the amount of heat that is transmitted through walls and roofs, the amount of longwave radiation that interacts with the outdoor environment, the amount of energy released by anthropogenic indoor activities (air conditioning, heating, and ventilation).

Average representative values of urban morphology are considered in the Base and Base-ALB Scenarios as in (Pichelli et al., 2014).

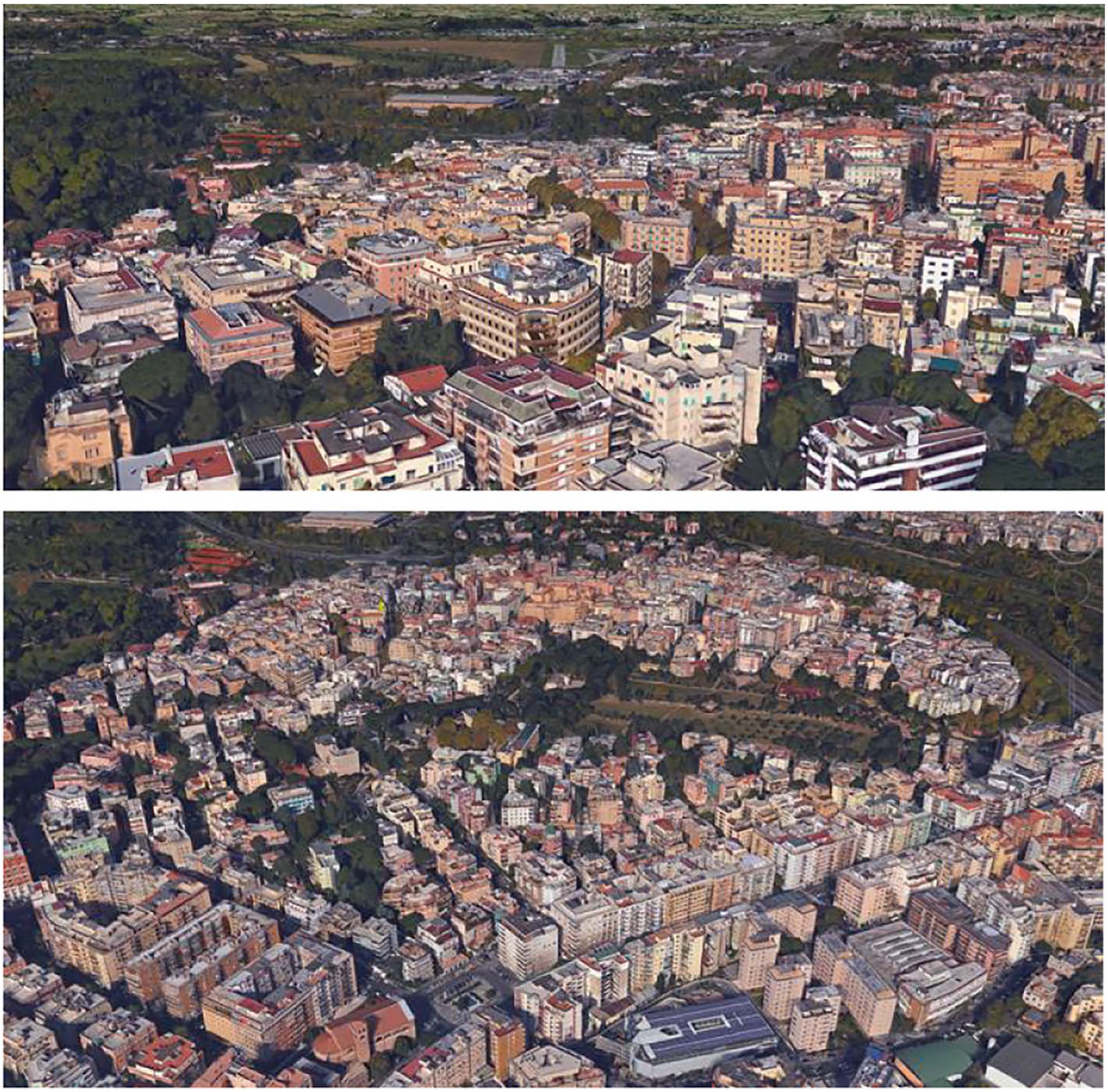

Fig. 4. Aerial views of the urban area.

In detail the height of buildings is considered as varying randomly between 5 m and 20 m; streets and buildings width is set between 20 m and 30 m and 13 m and 20 m.

The Morph Scenario and the Morph-ALB Scenario are characterized by the definition of the urban characteristics of the Trieste-Salario area (Fig. 4), that also includes the "Trieste-Salario" weather station (Fig. 5), as urban parameters for building heights, streets and buildings width in North-South and East-West directions.

An analysis of the urban structure and urban patterns has been carried out. The urban area is mainly characterized by 3 or 4 floors buildings, with an average height distribution set as in Table 3.

The parameters for streets and buildings width in North-South and West-East directions are set as 20 m and 20 m for streets and 19 m and 22 m for buildings.

The results from the Morph case are shown in Section 3.2 and are then compared with the Base case to check whether the simulated values are improved and closer to the measured ones. The results from the Morph-ALB case are then used to prove the effectiveness of the albedo increase against UHI.

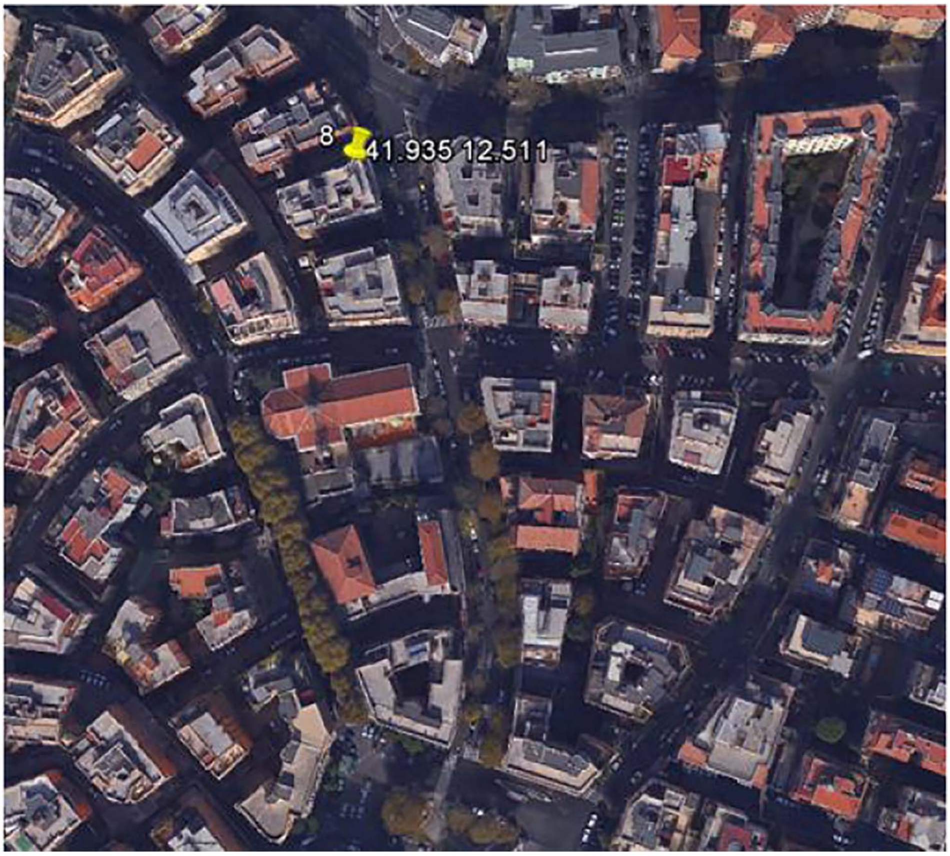

Fig. 5. Location of the “Trieste-Salario” weather station.

Table 3
Buildings height distribution.

Height	Percentage
5 m	0
10 m	10
15 m	30
18.5 m	60

2.5. Albedo enhancement

Albedo increase is the countermeasure to UHI that has been tested in the model. Two are the albedo enhancement cases: the Base-ALB Scenario and the Morph-ALB Scenario. In both cases the albedo of surfaces has been increased for High intensity Residential category. In Fig. 6 an extract of URBPARM.TBL file where the albedo of urban surfaces is set.

```
# Where there are multiple columns of values, the values refer, in
# order, to: 1) Commercial, 2) High intensity residential, and 3) Low
# intensity residential: I.e.:
# Index:        1          2           3
# Type: Commercial, Hi-dens Res, Low-dens Res

ALBR:  Surface albedo of roof [ fraction ]
ALBR: 0.20, 0.65, 0.20
ALBB:  Surface albedo of building wall [ fraction ]
ALBB: 0.20, 0.60, 0.20
ALBG:  Surface albedo of ground (road) [ fraction ]
ALBG: 0.20, 0.45, 0.20
```

Fig. 6. Extract of URBPARM.TBL file.

Table 4
Mean Absolute Error (MAE), Mean Bias Error (MBE), and Root Mean Square Error (RMSE) of observed and modeled 2-m air temperature (°C).

Weather station	1	2	3	4	5	6
MBE	− 1	− 1.9	− 1.1	− 2.1	− 1.27	− 1.8

3. Results and discussions

3.1. Model validation

The model has been evaluated by gathering as many data as possible from weather stations in Rome. The nine weather stations from Fig. 3 are considered for the validation. T2 values that is temperature at 2-m height have been compared. T2 has been compared for the validation because it is interesting for this work in terms of quantification and characterization of UHI.

Mean bias error has been calculated as the difference between simulated and recorded temperature as:

$$MBE = \frac{1}{n}\sum_{i=1}^{n} f_i - y_i \tag{2}$$

where f_i is the simulated and y_i the recorded value.

In Table 4 the error values for six reference weather stations are shown.

Pichelli et al. (2014) verified a general underestimation of vertical motions and an overestimation of the vertical transport of horizontal momentum from upper levels to low atmosphere. The overestimation was partially corrected by a local PBL scheme coupled with an advanced UCM and the model was validated.

The values of temperature are characterized by some underestimation as in Pichelli et al. (2014) but the error is considered acceptable, as in (Zhang and Zhaoxia, 2013). The model well reproduces the temperatures in the domain of interest, as further shown by the daily trend at Trieste-Salario (Fig. 7).

3.2. Urban morphology improvement

As described in Section 2.2 the urban morphology improvement has been implemented by the definition of urban parameters for building heights, streets and buildings width in North-South and East-West directions according to the urban characteristics of the Trieste-Salario area. To check the impact of urban morphology improvement on local simulation, the resulting values of T2 at Trieste-Salario have been compared to the previous results and to recorded values (Table 5). The errors show an improvement, even little, of the local temperature estimation.

Fig. 8 shows the simulated values from August 2nd at 12:00 to August 4th at 00:00 by BASE model and by MORPH model (dashed and dotted lines). The bold line represents the temperatures measured by the weather station. The MORHP values are closer to the recorded ones, especially at night. Radiation trapping and circulation in the canopy is better represented by MORPH model. However a higher improvement might be obtained by a deeper evaluation of buildings' characteristics (heat gains from occupants, solar energy transmitted through windows, infiltration, and air exchanges). This evaluation is beyond the scope of this paper, and is in process of investigation, since it involves energy and many other aspects, such as estimations of architecture parameters.

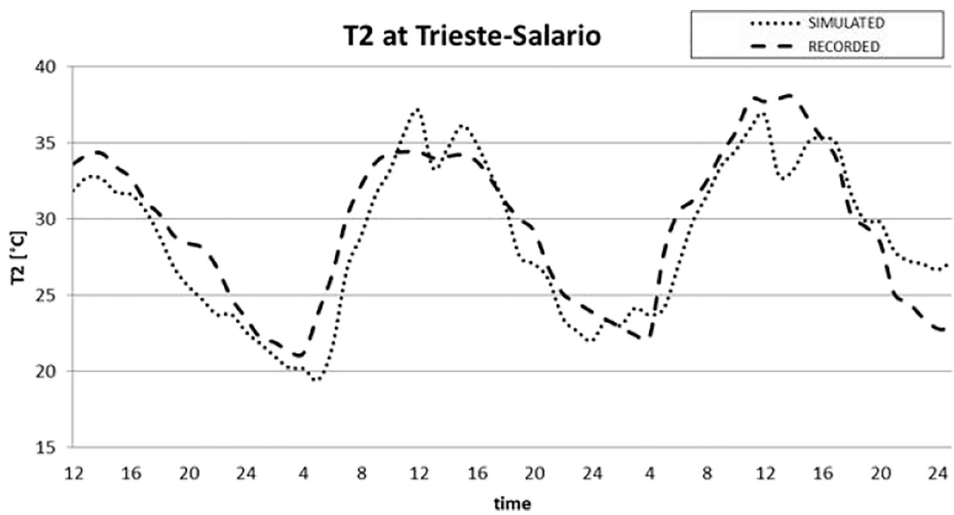

Fig. 7. Trend of simulated and recorded temperatures at Trieste-Salario weather station.

Table 5
Errors of Base Scenario and Morph Scenario at Trieste-Salario weather station.

Scenario	MBE
Base Scenario	− 1.27
Morph Scenario	− 1.02

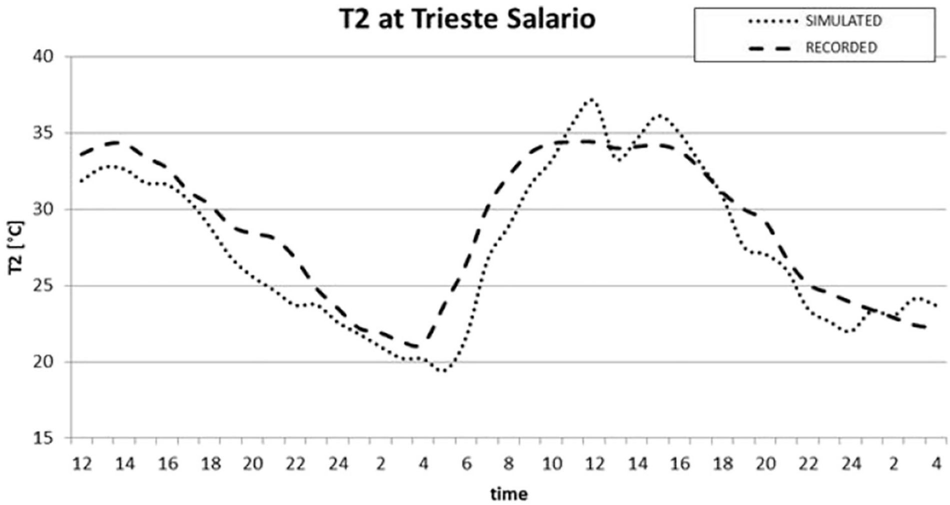

Fig. 8. Zoom on 36 h of simulation. Base, Morph Scenarios and recorded values at Trieste-Salario weather station.

3.3. UHI characterization

Some random points have been selected in the inner domain to find the difference between the 2-m air temperature of urban and rural areas. In Fig. 9, T2 in the reference urban grids (Urb1, Urb2, Urb3, Trieste-Salario as in Fig. 10) have been compared to T2 in the reference non-urban grids. The differences have been averaged for two main non-urban categories during 24 h: Land use category 2 in

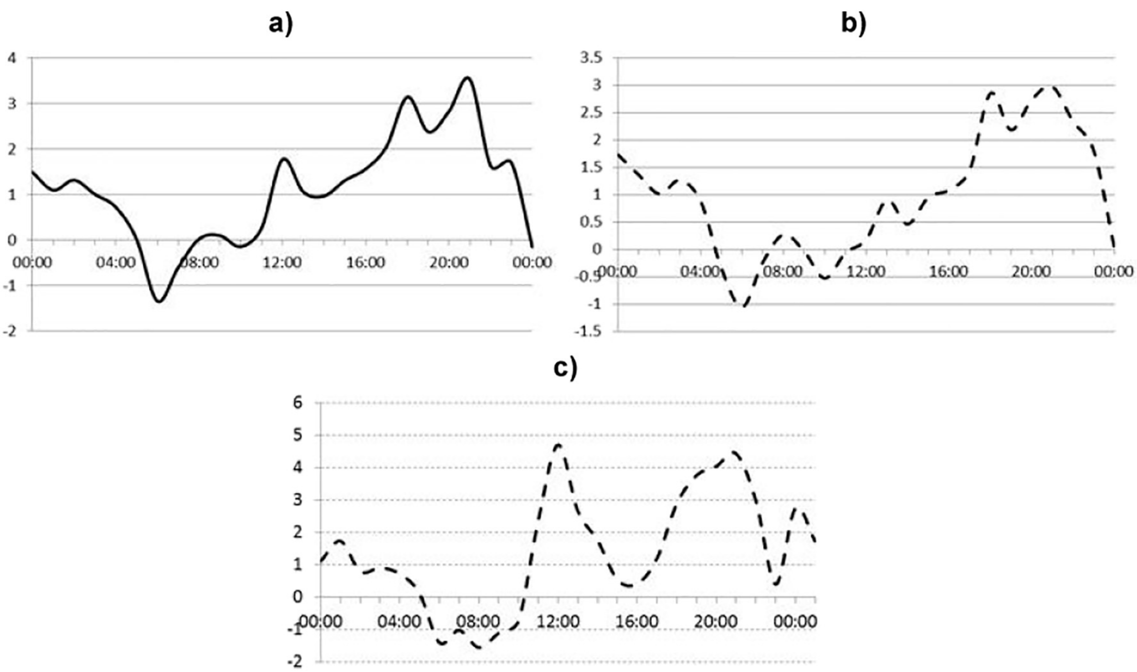

Fig. 9. Average UHI in the reference urban grids compared to a) Dryland Cropland and Pasture, b) Mixed Shrubland/Grassland and c) Mixed Shrubland/Grassland.

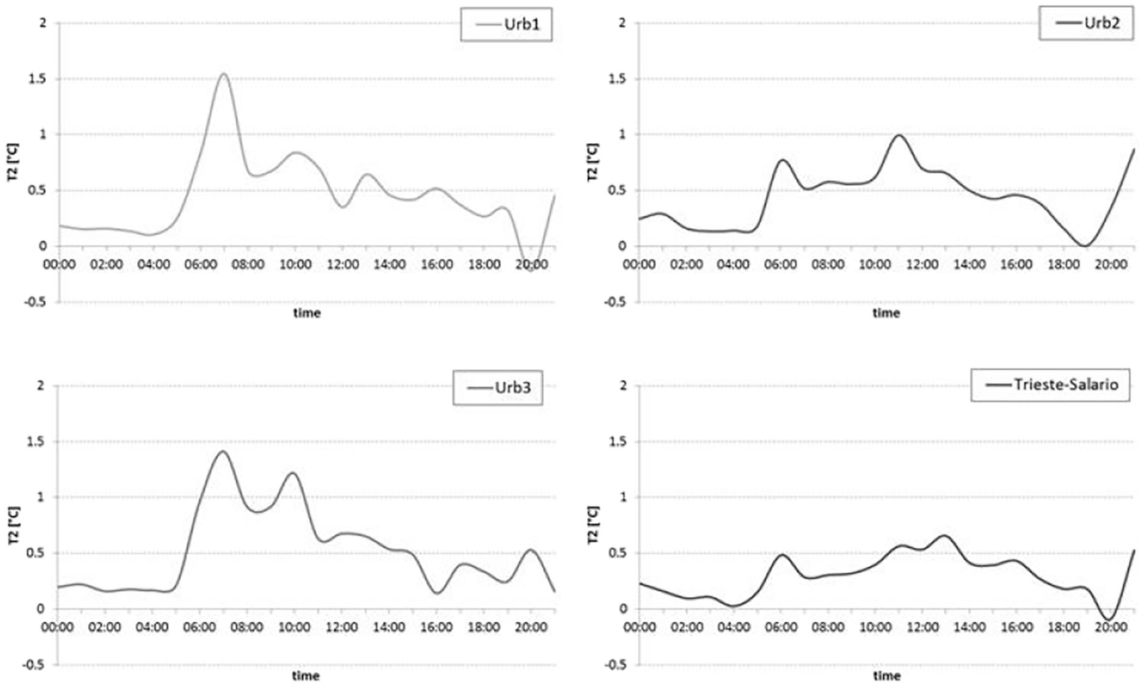

Fig. 10. Urban temperature reduction by urban albedo increase: ΔT(Base Scenario – Base-ALB Scenario) in the reference urban points.

a) - Dryland Cropland and Pasture - Land use category 6 in b) - Cropland/Woodland Mosaic - and Land use category 9 c) - Mixed Shrubland/Grassland.

In a) and b), the UHI phenomenon appears fully developed during the whole day from 12 to midnight, and is kept above 1 °C, with a maximum in the evening (between about 20:00 and 22:00). In c), the UHI is fully developed at 12:00, then decreases at 16:00 and fully re-develops in the evening (from 18:00).

As shown in Fig. 9, UHI can develop in different ways in grids that are further or closer to the urban grids. Grids in a) and b) are the closest to the urban area, as shown in Fig. 2. The distance to the urban area seems to influence the development of UHI. UHI develops after 12:00 and reaches the maximum in the evening in a) and b). UHI is very high at 12:00 in c) when the solar radiation is very high and the urban surfaces and thus the air temperature become very hot. After few hours of a decreasing ΔT, an increase of temperature happens in the urban area at about 18:00, due to the thermal storage of urban surfaces.

We consider the average and the max of these points as an average representation of UHI intensity for urban area. The maximum of the UHI intensity if found at 12:00 and it is about 5 °C. A 24-h average shows a 1.2 °C UHI intensity.

3.4. UHI mitigation

3.4.1. Base Scenario and Base-ALB Scenario

The increase of albedo in the urban area is simulated for Base Scenario in Base-ALB Scenario. Fig. 10 shows the ΔT of the reference urban points from August 3rd at 00:00 to August 4th at 00:00. It can be noticed that the temperature is decreased by albedo increase throughout the whole day and at night as well. Thus the decrease of thermal storage of surfaces is highly influent.

Fig. 11 shows the daily ΔT of the whole inner domain. The highest ΔT is at 7 am when it is up to 4 °C in some urban points in the Northern part of the urban area. The images show a ΔT of about 2 °C during the whole day in the urban area and also in a strip of land moving from towards South to towards East during the day. A ΔT of about 2 °C is also noticeable in some points at night time. An increase of temperature is also simulated in other points of the domain (up to 1 °C).

3.4.2. Morph Scenario and Morph-ALB Scenario

Fig. 12 shows the daily ΔT on the same urban points as Fig. 10 located in the urban area. ΔT is higher during the day, from 7 to 15, when the solar radiation is direct and strong. A lower ΔT is noticed at night time for Trieste-Salario, as in the previous simulations. For the two urban points Urb1 and Urb2, instead, an important decrease (more than 1.5 °C) is found at night time, too.

Fig. 13 shows the most meaningful ΔT on the whole inner domain.

The ΔT is positive at daytime in almost all the points of the domain. Some almost null values can be found and also some values a little lower than zero. At night time some negative values up to − 3 °C and some positive values up to 3.5 °C can be found. Thus, the albedo increase may lead to a positive effect on daytime temperature and both a positive and a negative night-time temperature in the investigated domain.

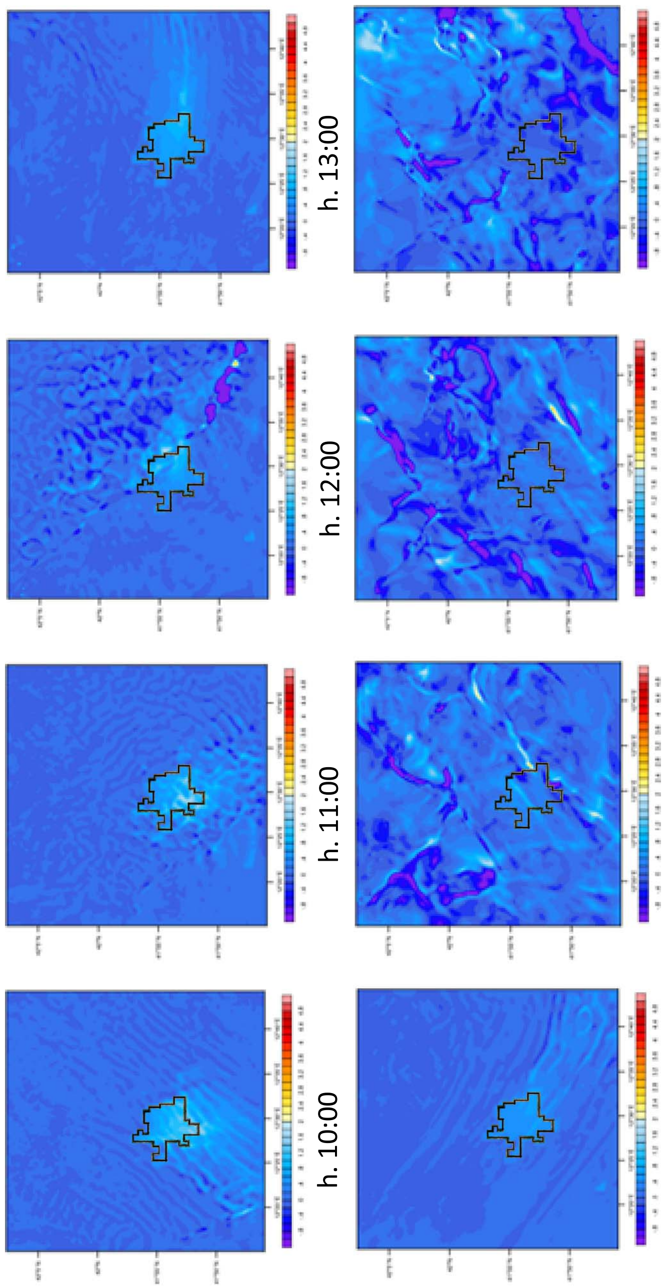

Fig. 11. Urban temperature reduction by urban albedo increase: ΔT (Base Scenario – Base-ALB Scenario) in the d04 domain (the black line delimits the urban area).

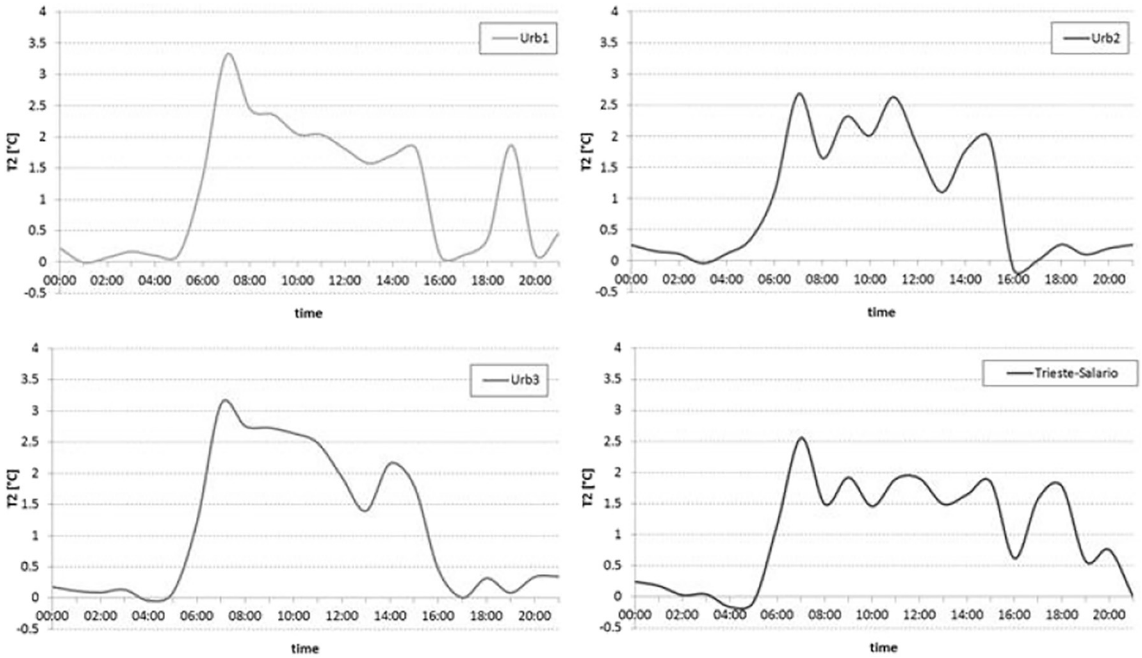

Fig. 12. Urban temperature reduction by urban albedo increase: ΔT (Morph Scenario – Morph-ALB Scenario) in the reference urban points.

3.5. UHI mitigation strategy implementation

In this section, actions for UHI reduction strategy development are proposed. Some possible interventions to increase the average albedo of surfaces and thus to increase the average urban albedo from 0.2 to 0.65, 0.6, 0.45 for roofs, walls and roads, respectively, are proposed. To this purpose, actions at building scale, including external surfaces of buildings, and at urban scale, including the urban surfaces such as streets, parking lots, yards and sidewalks are proposed.

Fig. 14 shows some views of the urban area of Rome of Trieste-Salario, Garbatella and Quartiere X Ostiense neighborhoods. These neighborhoods are representative of the metropolitan area of Rome that can be treated, keeping out the archaeological parks that are located within. Trieste-Salario neighborhood is characterized by intensive urbanization and large apartment buildings, once intended for government employees. Garbatella neighborhood is characterized by villas or small buildings of up to three stories, including significant green spaces that in the past were used for cultivation and newer large and tall buildings. Quartiere Ostiense neighborhood is characterized by the presence of industrial sites, including for example "I Mercati Generali" that used to be a very important commercial complex.

Building walls and roofs are considered the simplest and least-expensive surfaces for albedo modifications. As for buildings, a high-albedo paint could be applied on buildings such as 1, 2, 3, 4, 6, 10, 12 in Fig. 14. Many buildings are painted every 10 years: a high-albedo paint rather than a darker one can be applied, with no additional costs [Santamouris et al., 2004; Antonaia et al., 2016; Zinzi, 2016].

The albedo of roofs might also be changed using light-colored tiles [Rachi and Miyazaki, 2015; Pisello, 2015; Ferrari et al., 2016.] or light-colored rocks [Castaldo et al., 2015] on flat or gently sloped roofs such as in 2, 3, 4, 6, 9, 10, 11, 12.

Retro-reflective materials might also be used both for building façades, windows and for sloped roofs especially when the height of adjacent buildings is different such as in 2, 4, 11, 12 in Fig. 14 [Rossi et al., 2016; Fujita et al., 2014].

Roads, playgrounds and schoolyards as 5, 6, 7, 8 in Fig. 14 can be resurfaced or re-paved. In case of resurfacing to extend the life of street or parking areas a light colored aggregate is added, the albedo of a paved surface might be increased. For example asphalt might be replaced by concrete to increase the albedo. Or, cool pavement might be obtained with dark colored high albedo coating [Sreedhar and Biligiri, 2016; Kinouchi et al., 2004].

In addition to the mentioned considerations, the materials need to be selected in terms of efficiency, cost effectiveness, technical, maintenance and environmental problems. Furthermore, the proposed solutions must be carefully evaluated since the considered urban area is very complex. The very long history of the development of the city of Rome provides a beautiful heritage that needs to be protected. Many restrictions regulate urban, land use and infrastructure planning in the city of Rome (also Italian cities). A constraint in general is not necessarily an impediment, but it is considered as an extra step to take to get the permission to implement high albedo measures. Constraints can be identified as:

- architectural and artistic: high surveillance is foreseen on both public and private buildings for a good preservation of the architectural and artistic constraints, through the prior examination of the projects, the release of the opinion of competence and the

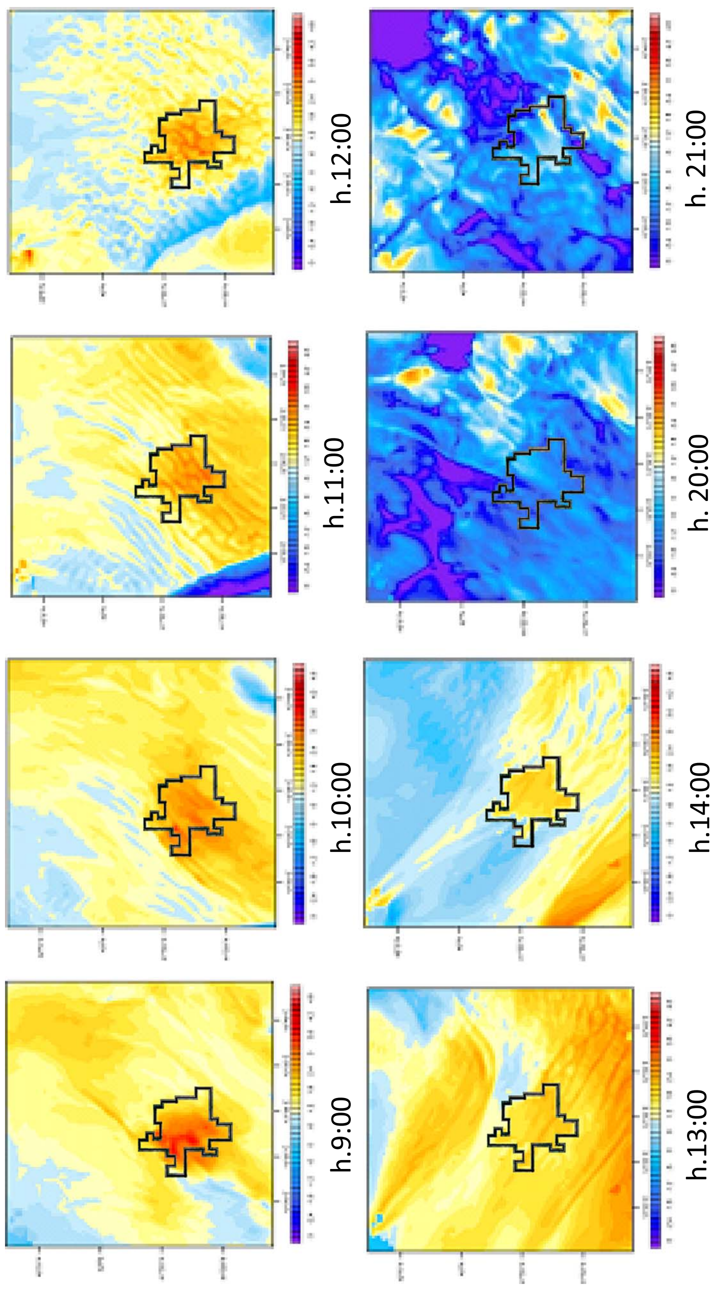

Fig. 13. Urban temperature reduction by urban albedo increase: ΔT (Morph Scenario − Morph-ALB Scenario) in the d04 domain (the black line delimits the urban area).

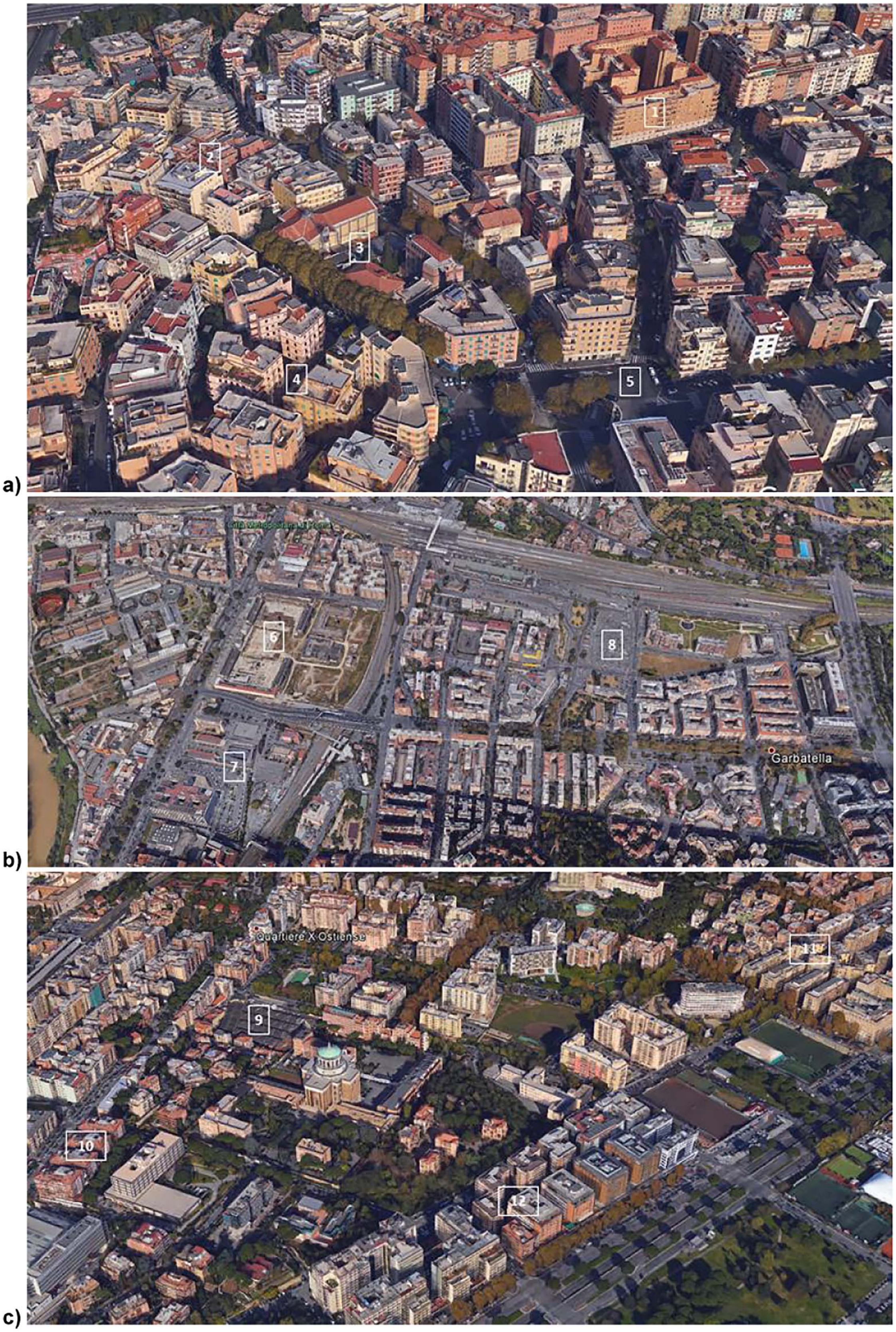

Fig. 14. Views of urban area of Rome. a) Trieste-Salario area; b) Garbatella neighborhood; c) Quartiere X Ostiense.

inspections during construction;
- monumental and archaeological: excavations, on land discoveries, archaeological sites, artistic, historical or religious monuments that represent testimonies and case studies of past ages;
- landscape and overall assets: safeguard measures and regulatory activities contribute to the active preservation of landscape heritage to avoid its defacement;
- geological: preventing from compromising natural resources (such as groundwater), ensuring the safety of the communities (such as avoiding to build in areas with hydrological instability or near active volcanoes)
- anthropogenic: imposed to ensure the proper functioning and security of man-made infrastructure, for example the constraints for airports, motorways, railways.

Constraints can be imposed either by the Ministry for Cultural Heritage, which requires the architectural and archaeological constraints, or the region, which defines geologic and infrastructure ones. But also the municipality imposes its constraints with the “City Plan”, that is the main instrument of the municipal urban planning: it is a planning instrument that regulates edificatoria activities within a municipal area, that every Italian town has to establish, in accordance with law.

4. Conclusions

We have simulated urban climate in the urban area of Rome (Italy) during cloudless, sunny days in summer 2013. The simulations have been implemented in four nested domains, the coarser one covering about 700 × 700 km^2. The inner domain d04 is focused on the area of Rome and the surrounding rural areas.

The Base Scenario simulation has been useful to validate the model.

In the Base-ALB Scenario the average albedo of the urban areas has been increased from 0.2 to 0.65, 0.6 and 0.45 for roofs, walls and roads respectively. The increase of albedo leads to a decrease of urban temperature at daytime and in general also at nigh time. In few points of the domain the temperature may be increased by 1 °C.

In the Morph Scenario, the morphology of the “Trieste-Salario" area is set as the urban dimensions and orientations of streets and buildings. An improvement of the simulation is observed, since the errors are decreased by 0.5 °C.

Furthermore, in the Morph-ALB Scenario the albedo has been increased. A higher improvement of urban temperature is noticed at day time, when the temperature can be decreased by 4 °C. At night time temperatures in some locations may be increased a little.

The paper demonstrates the effectiveness of albedo increase as a strategy to reduce UHI in the urban area of Rome both at day and at nigh time in some locations, with a specific attention to “Trieste-Salario” area. A further improvement is foreseen, by analyzing the whole urban area and the characteristics of different neighborhood that, because of the long history of the city of Rome have very different morphologies and urban dimensions. Such analysis will allow to investigate in an even more realistic way the effectiveness of urban albedo enhancement for the UHI reduction, and would represent an even more reliable instrument and support for urban planners, architects and government agencies for the implementation of policies to respond to and prepare for the impacts of climate change.

Acknowledgments

The authors acknowledge WU Weather Underground for weather data, NCAR for WRF-ARW source code, ECMWF for data analyses and CALCULQUEBEC Canada for computing resources. Hashem Akbari and Ali G Touchaei would like to acknowledge support from Natural Sciences and Engineering Research Council (NSERC) of Canada under discovery grant program.

References

Akbari, H., 2005. Energy Saving Potentials and Air Quality Benefits of Urban Heat Island Mitigation (PDF). (19 pp., 251K) Lawrence Berkeley National Laboratory.

Akbari, H., Sezgen, O., 1992. Analysis of energy use in building services of the industrial sector in California: two case studies. Energy Build. 19 (2), 133–141.

Akbari, H., Cartalis, C., Kolokotsa, D., Muscio, A., Pisello, A.L., Rossi, F., Santamouris, M., Synnefa, A., Wong, N.H., Zinzi, M., 2016. Local climate change and urban heat island mitigation techniques - the state of the art. J. Civ. Eng. Manag. 22 (1), 1–16.

Antonaia, A., Ascione, F., Castaldo, A., D'Angelo, A., De Masi, R.F., Ferrara, M., Vanoli, G.P., Vitiello, G., 2016. Cool materials for reducing summer energy consumptions in Mediterranean climate: in-lab experiments and numerical analysis of a new coating based on acrylic paint. Appl. Therm. Eng. 102, 91–107. (5 June 2016). (ISSN 1359-4311). http://dx.doi.org/10.1016/j.applthermaleng.2016.03.111.

Balsamo, G., Albergel, C., Beljaars, A., Boussetta, S., Brun, E., Cloke, H., ... Munoz Sabater, J., 2012. ERA-Interim/Land: A Global Land-surface Reanalysis Based on ERA-Interim Meteorological Forcing, ERA Report Series, ECMWF, Shinfield Park. Reading.

Buechley, R.W., Van Bruggen, J., Truppi, L.E., 1972. Heat island equals death island? Environ. Res. 5 (1), 85–92 (March 1972).

Castaldo, V.L., Coccia, V., Cotana, F., Pignatta, G., Pisello, A.L., Rossi, F., 2015. Thermal-energy analysis of natural “cool” stone aggregates as passive cooling and global warming mitigation technique. Urban Clim. 14 (2), 301–314. (December 2015). (ISSN 2212-0955). http://dx.doi.org/10.1016/j.uclim.2015.05.006.

Centers for Disease Control and Prevention, USA, 2004. MMWR Morb. Mortal. Wkly. Rep. 2004; 53(17). pp. 369–371.

Chen, F., Kusaka, H., Bornstein, R., Ching, J., Grimmond, C.S.B., Grossman-Clarke, S., Loridan, T., Manning, K.W., Martilli, A., Miao, S., et al., 2011. The integrated WRF/urban modelling system: development, evaluation, and applications to urban environmental problems. Int. J. Climatol. 31, 273–288.

Doulos, L., Santamouris, M., Livada, I., 2004. Passive cooling of outdoor urban spaces. In: The Role of Materials Solar Energy. Vo.l 77. pp. 231–249.

Dudhia, J., 1989. Numerical study of convection observed during the Winter Monsoon Experiment using a mesoscale two–dimensional model. J. Atmos. Sci. 46, 3077–3107.

Fallmann, J., Forkel, R., Emeis, S., 2016. Secondary effects of urban heat island mitigation measures on air quality. Atmos. Environ. 125 (Part A), 199–211. (January 2016). (ISSN 1352-2310). http://dx.doi.org/10.1016/j.atmosenv.2015.10.094.

Ferrari, C., Libbra, A., Cernuschi, F.M., De Maria, L., Marchionna, S., Barozzi, M., Siligardi, C., Muscio, A., 2016. A composite cool colored tile for sloped roofs with high ‘equivalent’ solar reflectance. Energy Build. 114, 221–226. (15 February 2016). (ISSN 0378-7788). http://dx.doi.org/10.1016/j.enbuild.2015.06.062.

Fujita, S., Inoue, T., Ichinose, M., Nagahama, T., Takakusa, S., 2014. Improvement of outdoor radiative environment by high-reflective facade: Effect of heat-shielding film with retro-reflective property in near infrared band. J. Environ. Eng. (Japan) 79 (696), 167–172 (February 2014).

Golden, J.S., 2010. The built environment induced urban heat island effect in rapidly urbanizing arid regions – a sustainable urban engineering complexity. Environ. Sci. 1 (2004 - Issue 4).

Hooshangi, H.R., Akbari, H., Touchaei, A.G., 2015. Measuring Solar Reflectance of Variegated Flat Roofing Materials Using Quasi-Monte Carlo Method (2015) Energy and Buildings, SI: Countermeasures to Urban Heat Island. Volume 114. pp. 234–240. (15 February 2016). https://www.usgs.gov. https://www.usgs.gov.

Janjic, Zavisa I., 1994. The Step–Mountain Eta Coordinate Model: Further developments of the convection, viscous sublayer, and turbulence closure schemes. Mon. Weather Rev. 122, 927–945.

Janjic, Z.I., 2002. Nonsingular Implementation of the Mellor-Yamada Level 2.5 Scheme in the NCEP Meso Model. NCEP Office Note No. 437. (61 pp.).

Kain, John S., 2004. The Kain–Fritsch convective parameterization: an update. J. Appl. Meteorol. 43, 170–181.

Kaufmann, R.J., Seto, K.C., Schneider, A., Liu, Z., Zhou, L., Wang, W., 2007. Climate response to rapid urban growth: evidence of a human-induced precipitation deficit. J. Clim. 20, 2299–2306. http://dx.doi.org/10.1175/JCLI4109.1.

Kinouchi, T., Yoshinaka, T., Fukae, N., Kanda, M., 2004. Development of cool pavement with dark colored high albedo coating. In: 5th Symposium on the Urban Environment 2004, pp. 207–210.

Kondo, H., Genchi, Y., Kikegawa, Y., Ohashi, Y., Yoshikado, H., Komiyama, H., 2005. Development of a multi-layer urban canopy model for the analysis of energy consumption in a big city: structure of the urban canopy model and its basic performance. Bound.-Layer Meteorol. 116 (2005), 395–421. http://dx.doi.org/10.1007/s10546-005-0905-5.

Kusaka, H., Kimura, F., 2004a. Thermal effects of urban canyon structure on the nocturnal heat island: numerical experiment using a mesoscale model coupled with an urban canopy model. J. Appl. Meteorol. 2004 (43), 1899–1910.

Kusaka, H., Kimura, F., 2004b. Coupling a single-layer urban canopy model with a simple atmospheric model: impact on urban heat island simulation for an idealized case. J. Meteorol. Soc. Jpn. 82 (1), 67–80.

Kusaka, H., Kondo, H., Kikegawa, Y., Kimura, F., 2001. A simple single-layer urban canopy model for atmospheric models: comparison with multi-layer and slab models. Bound.-Layer Meteorol. 101 (329–358), 2001.

Martilli, A., Clappier, A., Rotach, M.W., 2002. An urban surface exchange parameterization for mesoscale models. Bound.-Layer Meteorol. 104, 261–304.

Mlawer, E.J., Taubman, S.J., Brown, P.D., Iacono, M.J., Clough, S.A., 1997. Radiative transfer for inhomogeneous atmospheres: RRTM, a validated correlated–k model for the longwave. J. Geophys. Res. 102, 16663–16682.

Morini, E., Touchaei, A.G., Castellani, B., Rossi, F., Cotana, F., 2016. The impact of Albedo increase to mitigate the urban heat island in Terni (Italy) using the WRF model. Sustainability 2016 (8), 999. http://dx.doi.org/10.3390/su8100999.

Morini, E., Castellani, B., Presciutti, A., Filipponi, M., Nicolini, A., Rossi, F., 2017a. Optic-energy performance improvement of exterior paints for buildings. Energy Build. 139, 690–701.

Morini, E., Castellani, B., Presciutti, A., Anderini, E., Filipponi, M., Nicolini, A., Rossi, F., 2017b. Experimental analysis of the effect of geometry and façade materials on urban district's equivalent albedo. Sustainability (Switzerland) 9 (7), 245.

Morrison, H., Thompson, G., Tatarskii, V., 2009. Impact of cloud microphysics on the development of trailing stratiform precipitation in a simulated squall line: comparison of one– and two–moment schemes. Mon. Weather Rev. 137, 991–1007.

Peel, M.C., Finlayson, B.L., McMahon, T.A., 2007. Updated world map of the Köppen-Geiger climate classification. Hydrol. Earth Syst. Sci. 11, 1633–1644 (ISSN 1027-5606).

Pichelli, E., Ferretti, R., Cacciani, M., Siani, A.M., Ciardini, V., Di Iorio, T., 2014. The role of urban boundary layer investigated with high-resolution models and ground-based observations in Rome area: a step towards understanding parameterization potentialities. Atmos. Meas. Tech. 7, 315–332. www.atmos-meas-tech.net/7/315/2014/http://dx.doi.org/10.5194/amt-7-315-2014.

Pisello, A.L., 2015. Thermal-energy analysis of roof cool clay tiles for application in historic buildings and cities. Sustain. Cities Soc. 19, 271–280. (December 2015). (ISSN 2210-6707). http://dx.doi.org/10.1016/j.scs.2015.03.003.

Rachi, R., Miyazaki, H., 2015. Evaluation of clay tile roofing as a cool roof. In: (2015) Technology Reports of Kansai University. 57. pp. 75–80.

Ramamurthy, P., Li, D., Bou-Zeid, E., 2015. High-resolution simulation of heatwave events in New York City. Theor. Appl. Climatol. http://dx.doi.org/10.1007/s00704-015-1703-8.

Rosenfeld, A.H., Akbari, H., Bretz, S., Fishman, B.L., Kurn, D.M., Sailor, D., Taha, H., 1995. Mitigation of urban heat islands: materials, utility programs, updates. Energy Build. 22 (3), 255–265.

Rosenfeld, A.H., Akbari, H., Romm, J.J., Pomerantz, M., 1998. Cool communities: strategies for heat island mitigation and smog reduction. Energy Build. 28 (1), 51–62.

Rossi, F., Anderini, E., Castellani, B., Nicolini, A., Morini, E., 2015a. Integrated improvement of occupants' comfort in urban areas during outdoor events. Build. Environ. 93 (Part 2), 285–292. (November 2015). (ISSN 0360-1323). http://dx.doi.org/10.1016/j.buildenv.2015.07.018.

Rossi, F., Bonamente, E., Nicolini, A., Anderini, E., Cotana, F., 2015b. A carbon footprint and energy consumption assessment methodology for UHI-affected lighting systems in built areas. Energy Build. 2015.

Rossi, F., Morini, E., Castellani, B., Nicolini, A., Bonamente, E., Anderini, E., Cotana, F., 2015c. Beneficial effects of retroreflective materials in urban canyons: results from seasonal monitoring campaign. J. Phys. Conf. Ser. 655, 012012.

Rossi, F., Castellani, B., Presciutti, A., Morini, E., Anderini, E., Filipponi, M., Nicolini, A., 2016. Experimental evaluation of urban heat island mitigation potential of retro-reflective pavement in urban canyons. Energy Build. 126, 340–352. (15 August 2016). (ISSN 0378-7788). http://dx.doi.org/10.1016/j.enbuild.2016.05.036.

Ryu, Y.H., Bou-Zei, E., Wang, Z.H., Smith, J.A., 2016. Realistic representation of trees in an urban canopy model. Bound.-Layer Meteorol. 159, 193–220. http://dx.doi.org/10.1007/s10546-015-0120-y.

Sakka, A., Santamouris, M., Livada, I., Wilson, M., 2012. On the thermal performance of low income housing during heat waves. Energy Build. 49, 69–77 (June 2012).

Salamanca, F., Martilli, A., 2010. A new building energy model coupled with an urban canopy parameterization for urban climate simulations—part II. Validation with one dimension off–line simulations. Theor. Appl. Climatol. 99, 345–356.

Santamouris, M., 2016. Cooling the buildings – past, present and future. Energy Build. 128, 617–638. (15 September 2016). (ISSN 0378-7788). http://dx.doi.org/10.1016/j.enbuild.2016.07.034.

Santamouris, M., Adnot, J., Alvarez, S., Klitsikas, N., Orphelin, M., Lopes, C., Sanchez, F., 2004. Cooling the Cities - Rafraîchir les villes: Energy Efficient Cooling Systems and Techniques for Urban Buildings. Paris: Presses de l'Ecole des mines, 2004.

Sreedhar, S., Biligiri, K., 2016. Comprehensive laboratory evaluation of thermophysical properties of pavement materials: effects on urban heat island. J. Mater. Civ. Eng, 04016026. http://dx.doi.org/10.1061/(ASCE)MT.1943-5533.0001531.

Stewart, I.D., Oke, T.R., 2012. Local climate zones for urban temperature studies. Bull. Am. Meteorol. Soc. 93, 1879–1900.

Tan, J., Zheng, Y., Tang, X., Guo, C., Li, L., Song, G., Zhen, X., Yuan, D., Kalkstein, A.J., Li, F., Chen, H., 2010. The urban heat island and its impact on heat waves and human health in Shanghai. Int. J. Biometeorol. 54 (1), 75–84. (January 2010). http://dx.doi.org/10.1007/s00484-009-0256-x.

Tewari, M., Chen, F., Wang, W., Dudhia, J., LeMone, M.A., Mitchell, K., Ek, M., Gayno, G., Wegiel, J., Cuenca, R.H., 2004. Implementation and verification of the unified NOAH land surface model in the WRF model. In: 20th Conference on Weather Analysis and Forecasting/16th Conference on Numerical Weather Prediction, pp. 11–15.

Touchaei, A.G., Akbari, H., 2015. Evaluation of the seasonal effect of increasing the albedo on urban climate and energy consumption of buildings in Montreal. In: Urban Climate. Cooling Heat Islands. Volume 14. pp. 278–289 (Part 2, December 2015).

Wang, Z.H., Bou-Zeid, E., Smith, J.A., 2013. A coupled energy transport and hydrological model for urban canopies evaluated using a wireless sensor network. Q. J. R. Meteorol. Soc. 139, 1620–1635.

Wärmetechnische Grundlagen der Heizungs, 1982, 1982. Lüftungs- und Klimatechnik: mit 43 Tabellen.

WeatherSpark Average Weather for Rome, Italy. https://weatherspark.com/averages/32307/Rome-Lazio-Italy (web archive link, 10 January 2016) (accessed 01/10/2016).

WRF User Guide, 2009. Chapter 3: WRF Preprocessing System (WPS). land use and soil categories in the static data. http://www2.mmm.ucar.edu/wrf/users/docs/user_guide_V3/users_guide_chap3.htm.

Zhang, H., Zhaoxia, P., 2013. Examination of errors in near-surface temperature and wind from WRF numerical simulations in regions of complex terrain. Am. Meteorol. Soc. 2013 (28), 893–914.

Zinzi, M., 2016. Exploring the potentialities of cool facades to improve the thermal response of Mediterranean residential buildings. Sol. Energy 135, 386–397. (October 2016). (ISSN 0038-092X). http://dx.doi.org/10.1016/j.solener.2016.06.021.